Fuzzy Macromodel for Dynamic Simulation of Microelectromechanical Systems

Chun-Hsu Ko and Jin-Chern Chiou

***Abstract*—This paper proposes an efficient approach that consists of an experimental design and a fuzzy-logic model (FLM) to generate macromodels for the simulation of microelectromechanical systems. Firstly, in the present approach, a force macromodel is adapted to perform the coupled simulations. Then, an experimental design is utilized to reduce the number of data needed for macromodel identification, and an FLM is chosen to fit the data. The identification scheme involves cluster estimation to determine the FLM structure and backpropagation method to efficiently obtain the FLM structure parameters that lead to an accurate macromodel. In order to verify the accuracy of the macromodel, the approach has been applied to a magnetic microactuator. The simulation results show that the force macromodel yielded errors of less than 1.5% for a 5-μm displacement. Furthermore, the dynamic coupled simulation takes only several minutes. The results demonstrate the efficiency and effectiveness of the current approach.**

***Index Terms*—Coupled analysis, experimental design, fuzzy-logic model (FLM), macromodel, microactuator.**

I. Introduction

COMPUTATIONAL coupled analysis has attracted much attention in the design of microelectromechanical systems (MEMS), which require self-consistent solutions to coupled energy domains via nonlinear partial differential equations [1]. Numerical approaches, such as the finite-element method (FEM), can yield coupled quasi-static solutions [2]. However, the coupled simulations of fully meshed FEM models are usually time consuming, due to the fact that the models are usually with significant degrees of freedom (DOF). Furthermore, the coupled dynamic analysis of the system-level design requires many simulations, which are quite inefficient. Approaches using macromodels with relatively fewer DOFs (also called as reduced-order models) have been proposed to improve the efficiency of coupled dynamic analysis [3]–[6]. These macromodel approaches can accurately model the system by capturing the dominant dynamic behaviors and are effective for fast coupled system-level design.

In general, macromodel generation requires first finding the basis functions by using techniques, such as modal analysis [3], [4], singular-value decomposition [5], and neural-network method [6]. The macromodels are then built by adopting the generalized coordinates accompanied with these basis functions. It is possible to determine the macromodels by using analytical models [5], [6]. However, the use of analytic models usually demands assumptions, which may affect model accuracy and effectiveness. An attractive alternative is to build empirical macromodels using identification techniques [3], [4], [7]. The identified macromodel can be obtained via the fitting of a set of sampling data. This approach may demand many basis functions, leading to high input dimensions and also raising the complexity of data generation in running a large number of simulations [3]. Also, these previously proposed methods, such as multivariate polynomials [3] and neural network [4], have some drawbacks. The multivariate-polynomial model has low efficiency, and the neural-network approach cannot provide a meaningful interpretation of the network structure, which poses a difficulty in determining the structure. The macromodels in [3] and [4] are even with the differentiation of the identified energy model. Based on the discussions, it is imperative to achieve an efficient macromodel.

Fuzzy-logic models (FLMs), which can be used as structured numerical estimators, categorize the data obtained in experiments and then create meaningful fuzzy IF-THEN rules to form expert knowledge [8]. These FLMs combine fuzzy sets with fuzzy rules that have the capability to model the complex nonlinear behavior. Furthermore, the structure/parameter of the FLM has been efficiently identified by using the proposed learning approach, including cluster estimation, gradient descent, and the back-propagation method [9], [10]. Previous studies have demonstrated the feasibility of the Sugeno-type FLM in system modeling and control [10]–[13], which motivates us to further explore its possibility in building the MEMS macromodel.

This paper proposes an efficient approach to generating macromodels by using an experimental design and FLM. It is organized as follows. Section II introduces the macromodel approach for the MEMS systems. The fuzzy macromodel-generation method, which includes the experimental design for data sampling, an FLM to represent the data, and an efficient identification scheme for data fitting, is given in Section III. The example involving a magnetic microactuator, along with its corresponding static and dynamic simulations, are performed

Manuscript received April 27, 2004; revised December 9, 2004 and April 11, 2005. This work was supported by the Ministry of Economic Affairs, R.O.C., under Contract 92-EC-17-A-07-S1-0011, by the National Science Council of Taiwan, R.O.C., under Grant NSC 92-2215-E-009-009, and by the Brain Research Center, University System of Taiwan, under Grant 91B-711 and Grant 92B-711. This paper was recommended by Associate Editor T. H. Lee.

C.-H. Ko is with the Department of Computer Application Engineering, Far East College, Tainan County 744, Taiwan, R.O.C. (e-mail: koch.ece87g@nctu.edu.tw).

J.-C. Chiou is with the Department of Electrical and Control Engineering, National Chiao Tung University, Hsinchu 30010, Taiwan, R.O.C. (e-mail: chiou@cc.nctu.edu.tw).

Digital Object Identifier 10.1109/TSMCA.2005.855787

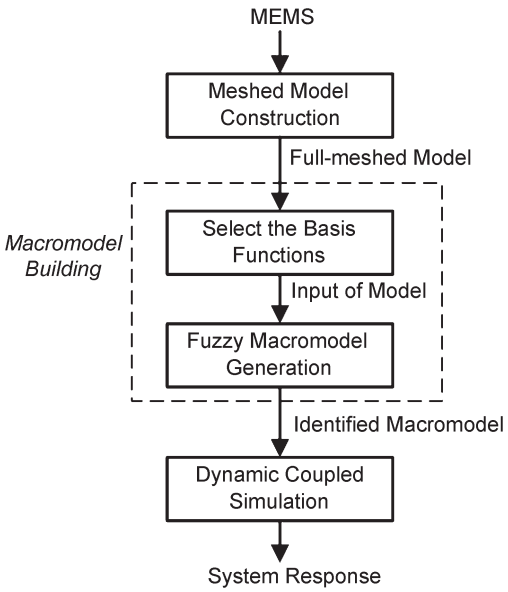

Fig. 1. Block diagram of the macromodel approach with FLM.

and reported in Section IV. Finally, the conclusion of the present paper are covered in Section V.

II. Macromodel Approach

Fig. 1 shows the procedure for the coupled dynamic analysis of MEMS using the macromodel approach with FLM. First, a fully meshed model of an MEMS is constructed by meshing the continuous distributed domains. Next, the degrees of freedom (DOF) of the system are reduced by selecting the basis functions, and inputs to the model are defined on the generalized coordinates. The identified macromodel is then built by using the FLM. Finally, a coupled dynamic simulation is performed based on the macromodel to yield the system response. From the procedure, to perform the simulation using the macromodel approach, we must first find the coupled dynamic equations of the system.

MEMS typically involve multiple energy domains, and their dynamic equations can be directly obtained from Lagrange's equations [14], which are given as

$$\frac{\mathrm{d}}{\mathrm{d}t}\left(\frac{\partial L}{\partial \dot{q}_i}\right) - \frac{\partial L}{\partial q_i} = 0 \tag{1}$$

where the Lagrangian $L(q, \dot{q}, t)$ is a function of the generalized coordinate q, their first derivatives $\dot{q}$, and time t. $L(q, \dot{q}, t)$ is defined by

$$L(q, \dot{q}, t) = T(q, \dot{q}, t) - U(q, \dot{q}, t) \tag{2}$$

where $T(q, \dot{q}, t)$ is the kinetic energy and $U(q, \dot{q}, t)$ the potential energy. By selecting the meshed nodal displacements u as the generalized coordinates, and assuming u as small displacements, the dynamic equations described in (1) then become

$$M\ddot{u} + Ku - F_m(u, t) = 0 \tag{3}$$

where M is the mass matrix defined on the mesh, K the stiffness matrix, and F_m the nodally defined actuation force. Note that the equations of motion of (3) are nonlinear and coupled. The meshed models for realistic calculation usually involve high DOFs, such that the users need to endure an intensive computation to obtain the simulation result. On the other hand, the macromodels have the capability to accurately simulate the system behavior of the modeled dynamic system with a few coupled equations. To build the macromodel, we select the n-dimensional generalized coordinates $q_i (i = 1, 2, \ldots, n)$, and n is much lower than the meshed model's DOFs, which yields

$$u = \sum_{i=1}^{n} q_i(t)\varphi_i \tag{4}$$

where $\varphi_i (i = 1, 2, \ldots, n)$ are the selected basis functions. These basis functions can be conveniently determined by using the natural modes from the modal analysis. The natural modes possess a useful property known as orthogonality. Equation (3) then becomes

$$\ddot{q}_i + \omega_i^2 q_i = \varphi_i^{\mathrm{T}} F_m(q, t) \tag{5}$$

where $\omega_i (i = 1, 2, \ldots, n)$ are the natural frequencies and $q = [\, q_1 \quad q_2 \quad \ldots \quad q_n \,]^{\mathrm{T}}$. Note that the electromagnetic force F_m for actuating MEMS can be expressed as

$$F_m(q, t) = I^2(t) f_{\mathrm{m}}(q) \tag{6}$$

where $I(t)$ is the input current that depends on time t in current-controlled devices and $f_{\mathrm{m}}(q)$ is the magnetic force resulting from the unit input current. Substituting (6) into (5), we have

$$\ddot{q}_i + \omega_i^2 q_i = I^2(t) p_i(q) \tag{7}$$

where $p_i(q) = \varphi_i^{\mathrm{T}} f_{\mathrm{m}}(q)$ is the generalized force, referred to as the force macromodel.

On the other hand, the reduced-order dynamic equations can also be directly derived from (1) using the magnetic coenergy [3]

$$\ddot{q}_i + \omega_i^2 q_i = I^2(t) \frac{\partial u_{\mathrm{m}}^*(q)}{\partial q_i} \tag{8}$$

where $u_{\mathrm{m}}^*(q)$ is the magnetic coenergy resulting from the unit input current, referred to as the energy macromodel, and its differentiation $\partial u_{\mathrm{m}}^*(q)/\partial q_i$ represents the generalized force.

Equations (7) and (8) are both reduced-order equations for different forms of magnetic macromodels, leading to different computation procedures. Here, the force macromodel $p_i(q)$ first requires the evaluation of the magnetic force in displacement (u) space, and is then obtained by projecting the magnetic force onto the generalized q space with the inner product of the magnetic force and the normal modes. The energy macromodel $u_{\mathrm{m}}^*(q)$, on the other hand, requires the coenergy function to

be established in q's space, and the generalized force is then obtained with the differentiation of the coenergy function.

To increase the efficiency in performing the coupled dynamic-system simulations in (7) and (8), macromodels in analytical form are required. In order to generate macromodels, it is necessary to select the basis functions that are significantly contributed to the system dynamic behavior. The selection process begins with the typical displacement u_{s}, which contains information on the amplitude for each basis function [3], [4]. The displacement is calculated from the coupled quasi-static analysis with FEM software, such as ANSYS (ANSYS, Inc., Canonsburg, PA. http://www.ansys.com). Using the n_{s} (about 30) modes of the lower natural frequency as the basis functions, the displacement can be expanded with the coefficients y_i as

$$u_{\mathrm{s}} \approx \sum_{i=1}^{n_{\mathrm{s}}} y_i \varphi_i. \tag{9}$$

Note that (9) is an overdetermined system requiring a least-square solution. The orthogonal-triangular (QR) factorization algorithm is adopted to yield the coefficients y_i [15]. The displacements of the modes can then be calculated by indicating important modes. Furthermore, the magnitudes of the coefficients y_i are used to predict the relative ranges of q_i for the input domain of the macromodel. Once the basis functions and the estimation range are determined, the fuzzy model-identification method can be used to generate the nonlinear macromodel.

III. Fuzzy Macromodel Generation

The fuzzy macromodel generation with the identification technique includes data sampling, FLM selection, and FLM identification, which are described below.

A. Data Sampling

The data for macromodel generation are the generalized coordinates q as the input variables and the generalized force or coenergy as the output. Note that input-data selection is important since it will affect both the reliability of the macromodel and the number of simulation runs. Thus, proper design of the simulation experiments is imperative. The experimental design takes certain values, called levels, for every input variable. The levels are used to adequately span the input range. The number of input data depends on the input variables and levels. Data with more input variables (i.e., more basis functions) and levels lead to more accurate macromodels, but also increase the difficulty in data selection. For example, n input variables and m levels produce a total of n^m runs for all the combinations, which shows the exponential increase in data number. Hence, an efficient experimental design is needed to obtain accurate results from a minimum number of computer runs.

To achieve this objective, Taguchi's method is proposed [16]. This method provides a predefined set of orthogonal tables that contain fractional orthogonal designs. For example, two-level L_4, L_{12}, and L_{16} arrays [16] allow 3, 11, and 15 inputs to be evaluated with only 4, 12, and 16 design points, rather than the exponential 2^3, 2^{12}, and 2^{16}.

B. FLM Selection

In Sugeno-type FLM, the ith rule is described as follows.

If x_1 is F_{i1}, and x_2 is F_{i2}, $\cdots$ and x_n is F_{in}, then the role output is

$$y_i(x_1, x_2, \ldots, x_n) = p_{i0} + p_{i1}x_1 + p_{i2}x_2 + \cdots + p_{in}x_n$$

where $x_j (j = 1, 2, \ldots, n)$ is the input variable, F_{ij} the fuzzy set, and output y_i an internal function with parameters $P_{i0}, P_{i1}, \cdots, P_{in}$. The Gaussian-type membership function μ_{Fij} for the input variable x_j can be expressed as

$$\mu_{Fij}(x_j) = \exp\left[-\frac{1}{2}\left(\frac{x_j - c_{ij}}{\sigma_{ij}}\right)^2\right] \tag{10}$$

where c_{ij} and σ_{ij} are, respectively, the location and shape parameters. Then, by using the product operator to represent the and operator in the rules, the weight for each rule's output becomes

$$w_i = \exp\left[-\frac{1}{2}\sum_{j=1}^{n}\left(\frac{x_j - c_{ij}}{\sigma_{ij}}\right)^2\right]. \tag{11}$$

Finally, the output of the FLM is inferred by taking the weighted average of the rule's outputs. For an FLM with r rules, the output can be expressed as

$$y = \sum_{i=1}^{r} v_i y_i, \qquad \text{with } v_i = \frac{w_i}{\sum_{i=1}^{r} w_i}. \tag{12}$$

With the energy macromodel described in (8), the generalized force can be obtained by differentiating the fitted coenergy function. The differentiation of the FLM output can be analytically derived as

$$\frac{\partial y}{\partial x_j} = \sum_{i=1}^{r} v_i \left(\frac{-(x_j - c_{ij})}{\sigma_{ij}^2} + \sum_{k=1}^{r}\frac{v_k(x_j - c_{ij})}{\sigma_{kj}^2} + p_{ij}\right). \tag{13}$$

The total number of membership functions and internal function parameters in the FLM to be determined is $r \times (3 \times n + 1)$. Minimization of the squaring errors between the sampling data and the calculated FLM outputs, in turn, determines these parameters.

C. FLM Identification

For a set of sampling data $(x_{1k}, x_{2k}, \ldots, x_{nk}, y_k)$, the accuracy of the FLM is given by the multiple correlation coefficient R^2 [10], which is defined as

$$R^2 = 1 - \frac{\sum_{k=1}^{m} (\hat{y}_k - y_k)^2}{\sum_{k=1}^{m} (\hat{y}_k - \overline{y})^2} \tag{14}$$

where $\hat{y}_k$ is the output of the macromodel, $\overline{y}$ the mean of the output of the sampling data, and m the total number of data sets. When $R^2 = 1$, it means that the model fits every sampling data point perfectly. The primary goal of FLM identification is to maximize R^2 to 1, and, thus, the resulting FLM makes accurate predictions of the input domain.

There are two major tasks in identifying an FLM for a system: structure and parameter identification [17]–[19], each of which consists of a premise and a consequence part. To identify the FLM parameters with an optimal structure accurately, we partition the available data into training and testing data. An efficient identification approach involving cluster estimation, gradient-descent, and backpropagation method is then utilized to identify intermediate FLMs with various structures using the training data. The decision rule seeks maximal multiple correlation coefficients among the intermediate FLMs and the testing data to achieve an optimal structure. Thus, the resulting macromodel not only fits the training data well, but also makes accurate predictions.

The cluster-estimation method [9], [10] is used here for the coarse tuning process of the FLM identification algorithm. Data-point potential measure is used to locate the cluster centers, defined as

$$V_i = \sum_{k=1}^{m} \exp\left(-\frac{4}{r_a^2}\|x_i - x_k\|^2\right) \tag{15}$$

where $\|.\|$ denotes the Euclidean distance and r_a a positive constant used to define the effective radius of a neighborhood. The data points with higher potentials are chosen as cluster centers. Each cluster center is, in essence, a prototypical data point that exemplifies a characteristic behavior of the system [9]. Hence, each cluster center can be used as the basis of a rule-describing system behavior, and the number of fuzzy rules will be equal to that of the cluster centers.

When the fuzzy structure is determined, parametric identification of a fuzzy model based on the gradient-descent and backpropagation methods is then conducted. The output of the FLM is calculated and internal parameters are updated by the instantaneous error between the FLM output $\hat{y}_k$ and the current training data output y_k. Here, we minimize the square of the instantaneous error with respect to the unknown parameters p_{i0}, p_{ij}, c_{ij}, and σ_{ij} of the internal functions and membership functions, i.e.,

$$E_k = \frac{1}{2}(\hat{y}_k - y_k)^2 = \frac{1}{2}e_k^2. \tag{16}$$

By applying the chain rule on (16), we can obtain the equations for updating the estimates of the unknown parameters p_{i0}, p_{ij}, c_{ij}, and σ_{ij} as

$$p_{i0}(k+1) = p_{i0}(k) - \alpha_0 v_i(k) e_k \tag{17}$$

$$p_{ij}(k+1) = p_{ij}(k) - \alpha_1 v_i(k) e_k x_j \tag{18}$$

$$c_{ij}(k+1) = c_{ij}(k) - \alpha_2 v_i(k) e_k \times [y_i(k) - y_k] \frac{x_j - c_{ij}(k)}{\sigma_{ij}^2(k)} \tag{19}$$

$$\sigma_{ij}(k+1) = \sigma_{ij}(k) - \alpha_3 v_i(k) e_k \times [y_i(k) - y_k] \frac{[x_j - c_{ij}(k)]^2}{\sigma_{ij}^3(k)}. \tag{20}$$

The gradient-descent method is used to minimize the instantaneous error. Since this method is basically a kind of hill-climbing technique, it runs the risk of being trapped in a local minimum, where every small change in synaptic parameters p_{i0}, p_{ij}, c_{ij}, and σ_{ij} would increase the square-error function E_k. Therefore, initial parameter estimation is crucial when this method is used. Here, the initial parameter estimations c_{ij} and p_{i0} are the coordinates of the ith cluster center $(x_{1i}^*, x_{2i}^*, \ldots, x_{ni}^*, y_i^*)$, and the parameter σ_{ij} is defined as the distance with the constant r_a, i.e., $\sigma_{ij} = l \times r_a$. By using the results obtained in [10], parameter l is set to $3/(4\sqrt{2})$, and p_{ij} to zero. The method is used repeatedly to update the model parameters until $R^2 \geq R_{\min}^2$. Note that the criterion $R^2 \geq R_{\min}^2$ is to ensure the accuracy of the FLM.

Finally, intermediate FLMs with various structures are built from the training data by using the identification method described above. A multiple correlation coefficient R_{search}^2 (e.g., 0.99) is specified for fast establishing the intermediate FLMs. The testing data are used to evaluate the accuracy of the intermediate FLMs by employing the multiple correlation coefficients recorded as R_{test}^2. The FLM structure with the highest R_{test}^2 is then chosen as the optimal structure. We further use the training and testing data with a larger multiple correlation coefficient R_{goal}^2 (e.g., 0.9999) than R_{search}^2 to identify the accurate FLM with the optimal structure.

Based on the discussion above, the FLM identification algorithm is developed and stated as follows.

FLM Identification Algorithm:

Step 1) Specify the input variables $x_1, x_2, \ldots, x_n$, and the output variable y.
Step 2) Provide training and testing data.
Step 3) Give the maximum number of rules $r_{\max}$ to establish the intermediate FLMs, and the multiple correlation coefficients R_{search}^2 and R_{goal}^2.
Step 4) Begin the search algorithm and set the fuzzy rule number $r = 1$.
Step 5) Use the cluster-estimation method to search for the constant r_a for building the FLM structure with r rules and the initial parameters p_{i0}, p_{ij}, c_{ij}, and σ_{ij}.

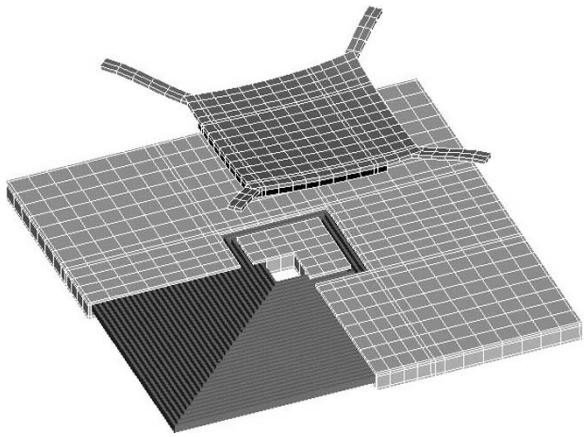

Fig. 2. Quasi-static displacement of asymmetric suspended plate with 36-mA actuation.

TABLE I
MODE CONTRIBUTIONS TO THE DISPLACEMENT OF THE PLATE CENTER

Mode Number	Contribution (μm)
1	-5.2941
3	0.1789
2	0.0569
6	0.0142
8	0.0044
10	0.0031
7	0.0021
12	0.0021
5	0.0014
9	-0.0013

Step 6) Calculate the FLM output y_k with the training data, and the instantaneous error e_k. Perform back-propagation to refine the parameters p_{i0}, p_{ij}, c_{ij}, and σ_{ij} with the gradient-descent method.

Step 7) Calculate the training correlation coefficient R^2. If R^2 is less than R^2_{search}, go to Step 6) for the next iteration; otherwise, test the FLM using the testing data and record the testing correlation coefficient as $R^2_{\text{test}}(r)$.

Step 8) Set $r = r + 1$, if r is less than or equal to $r_{\max}$, go to Step 5); otherwise, select the rule number r that corresponds to the maximum test correlation coefficient $R^2_{\text{test}}(r)$ as the optimal rule number r_{opt}.

Step 9) Set-up all available data in Step 2) as new training data and R^2_{goal} as the convergence correlation coefficient. Identify the optimal FLM with r_{opt} rules and output its parameters.

IV. SIMULATIONS AND RESULTS

In order to demonstrate the efficiency of the proposed approach, the macromodeling process was applied to a magnetic microactuator containing a magnetic core and a deformable structure [20]–[22]. The structure of the microactuator was shown in Fig. 2. The magnetic microactuator had an asymmetric $625 \times 625 \times 5$ μm plate suspended from four beams 50-μm wide by 5-μm thick, the shortest of which was 150-μm high, the tallest 300-μm high, and the others 200- and 250-μm high. A $500 \times 500 \times 5$ μm permalloy panel was attached under the plate at the corner near the shortest support beam, and an electromagnet consisting of a 32-turn coil and an enclosed core was placed underneath, separated from the permalloy plate by a 16-μm gap. Due to the unequal beam length and the off-center magnetic force, this structure displaced, bent, and tilted upon application of electrical current.

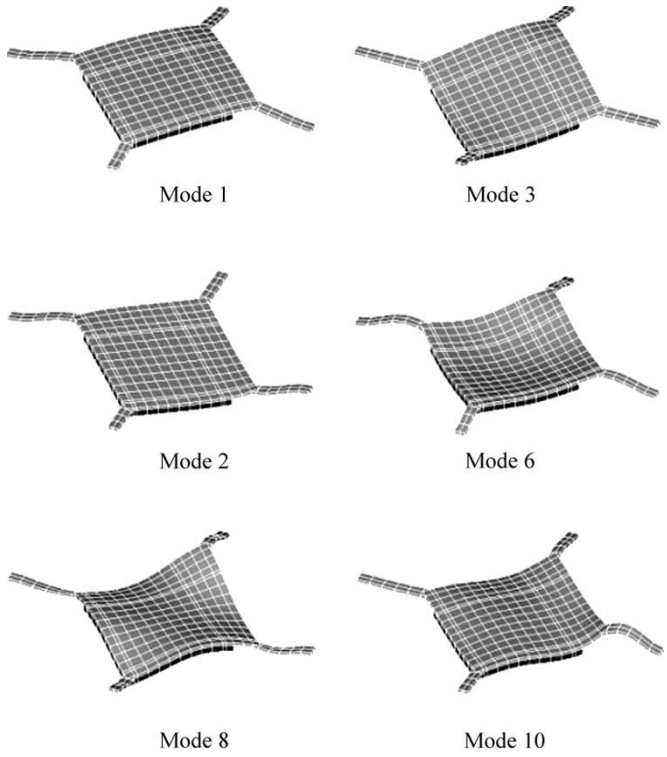

Fig. 3. Mode shapes used as the basis functions.

TABLE II
MODE PARAMETERS

Mode Number	Frequency (kHz)
1	16.3
3	53.5
2	34.4
6	192.5
8	266.3
10	363.1

In the simulation, we used the ANSYS software to construct a three-dimensional (3-D) model by meshing a magnetic microactuator to create structural and magnetic FEM models. The structural finite-element mesh, which had its thickness magnified by four times for clarity, comprised 411 solid elements with a total of 799 nodes, and the magnetic FEM model contained 17 408 eight-node brick elements for a total of 19 602 nodes. An equilibrium displacement was obtained via the quasi-static magnetostructural simulation, with the resulting deformation depicted in Fig. 2.

The first thirty mode shapes of the structural FEM model are determined using modal analysis. We projected the quasi-static solution onto the mode shapes using QR factorization. Table I lists the ten most significant modes contributing to this

TABLE III
$L_{25}(5^6)$ ORTHOGONAL ARRAY

Setting	A	B	C	D	E	F
1	1	1	1	1	1	1
2	1	2	2	2	2	2
3	1	3	3	3	3	3
4	1	4	4	4	4	4
5	1	5	5	5	5	5
6	2	1	2	3	4	5
7	2	2	3	4	5	1
8	2	3	4	5	1	2
9	2	4	5	1	2	3
10	2	5	1	2	3	4
11	3	1	3	5	2	4
12	3	2	4	1	3	5
13	3	3	5	2	4	1
14	3	4	1	3	5	2
15	3	5	2	4	1	3
16	4	1	4	2	5	3
17	4	2	5	3	1	4
18	4	3	1	4	2	5
19	4	4	2	5	3	1
20	4	5	3	1	4	2
21	5	1	5	4	3	2
22	5	2	1	5	4	3
23	5	3	2	1	5	4
24	5	4	3	2	1	5
25	5	5	4	3	2	1

TABLE IV
$L_{16}(4^5)$ ORTHOGONAL ARRAY

Setting	A	B	C	D	E, F
1	1	1	1	1	1
2	1	2	2	2	2
3	1	3	3	3	3
4	1	4	4	4	4
5	2	1	2	3	4
6	2	2	1	4	3
7	2	3	4	1	2
8	2	4	3	2	1
9	3	1	3	4	2
10	3	2	4	3	1
11	3	3	1	2	4
12	3	4	2	1	3
13	4	1	4	2	3
14	4	2	3	1	4
15	4	3	2	4	1
16	4	4	1	3	2

deformation and their contributions to the displacement of the plate center. To obtain a reduced-order model, the six dominant modes, shown in Fig. 3, were selected as the basis functions for computing system response. Table II lists the frequencies for each of the selected modes.

The proposed macromodel-generation approach was used to build the nonlinear magnetic macromodel. The first six modes were taken as the shape functions along with their contributions as the input ranges of the macromodel. By setting five levels for each factor and using the orthogonal table $L_{25}(5^6)$ from Taguchi's method, shown in Table III, we obtained training data through performing 25 simulations of magnetic force and coenergy. Meanwhile, the orthogonal table $L_{16}(4^5)$ containing 16 simulations was used for obtaining the testing data, as shown in Table IV. The testing-data levels were determined by taking the four middle points of the five levels in the training data. Note that table $L_{16}(4^5)$ was for an experimental design of five factors. To permit experimenting on six factors with a table of five factors, we combined minor factors (the fifth and sixth factors) into a compound factor. Finally, the FLM identification algorithm was used to obtain the identified macromodels.

TABLE V
COMPUTATION TIMES FOR MACROMODEL GENERATION

Generation Procedure \ Macromodel	Force Macromodel	Energy Macromodel
Quasi-Static Analysis (s)	4320	4320
Modal Analysis (s)	10	10
Modes Selection (s)	30	30
Data Sampling (s)	10660	10824
FLM Identification (s)	148	16
Total Time (h)	4.21	4.22

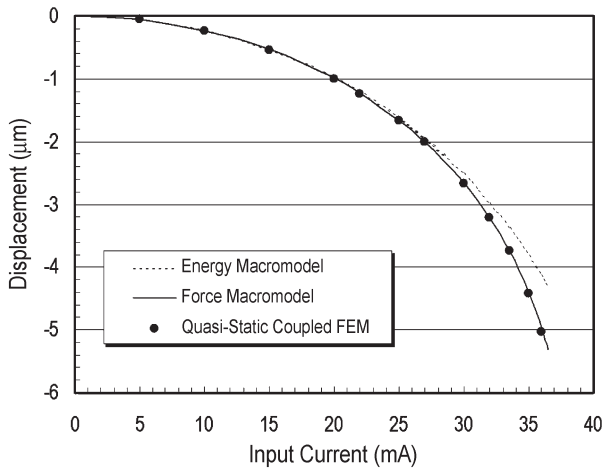

Fig. 4. Comparison of the solutions of the plate-center displacement by using force macromodel, energy macromodel, and quasi-static coupled FEM.

Table V shows the macromodeling computation times for force and energy macromodels run on a Pentium-III 850-MHz microprocessor. The total computation time was almost the same for both macromodeling approaches, approximately within 4.5 h for the complex example. We found that the data-sampling procedure took most of the macromodel-generation time. Note that the total run time would have been longer in the absence of the experimental design. Hence, the experimental design was effective in reducing the total required run time. Meanwhile, FLM identification took only a few minutes, demonstrating the efficiency of the proposed identification approach.

To check the accuracy of the fitted macromodel, the quasi-static case was firstly performed by setting the time derivatives

TABLE VI
MACROMODEL ACCURACY IN COUPLED QUASI-STATIC SIMULATIONS

Current (mA)	FEM Coupled Quasi-Static Solution (μm)	Force Macromodel		Energy Macromodel	
		Solution (μm)	Error (%)	Solution (μm)	Error (%)
5	-0.057	-0.057	-0.20	-0.055	-3.27
10	-0.231	-0.231	-0.23	-0.224	-3.15
15	-0.536	-0.534	-0.28	-0.520	-3.02
20	-0.996	-0.993	-0.31	-0.967	-2.98
25	-1.664	-1.660	-0.27	-1.606	-3.37
30	-2.661	-2.657	-0.16	-2.519	-5.33
35	-4.416	-4.395	-0.47	-3.821	-13.48
36	-5.034	-4.961	-1.43	-4.142	-17.72

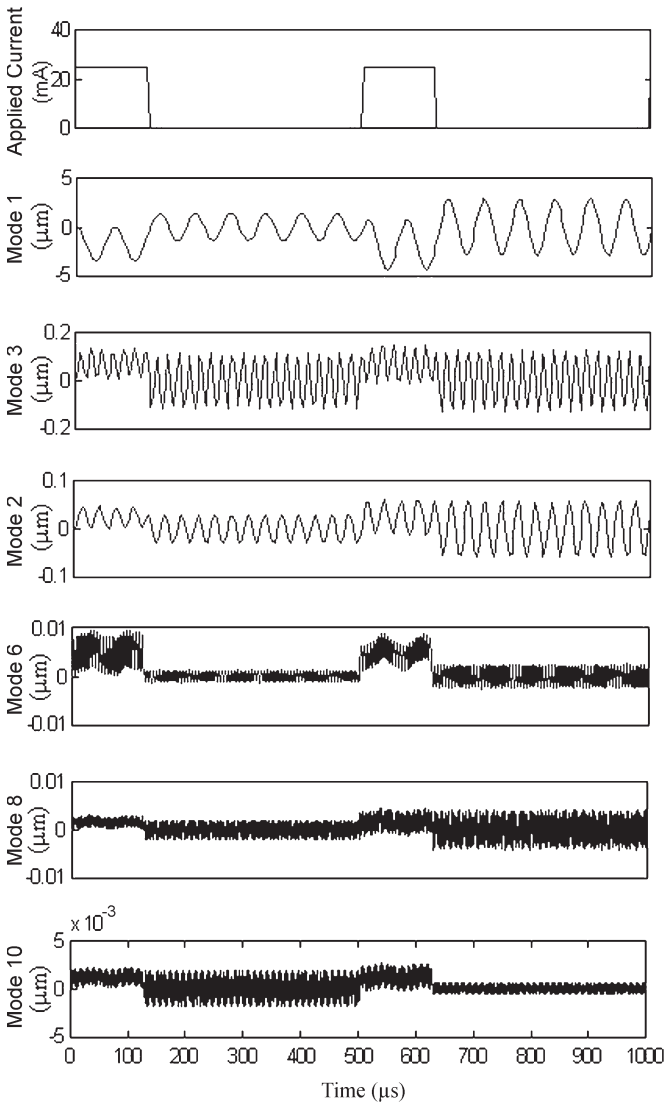

Fig. 5. Response to a 25-mA square wave with a 125-μs hold and a 500-μs period.

to zero in the dynamic equations of motion. The solution was obtained by solving a set of coupled algebraic equations, and it agrees well with the solution of the coupled quasi-static FEM simulation. Fig. 4 shows the comparison of the solutions of plate-center displacement, and Table VI presents the accuracy of the macromodels. We found that the force macromodel yields an error of less than 1.5% for a 5-μm displacement, demonstrating that the proposed force-macromodeling approach was very effective. But the solution from the energy macromodel shows a much larger error generated by using the differentiation of the fitted-energy macromodel.

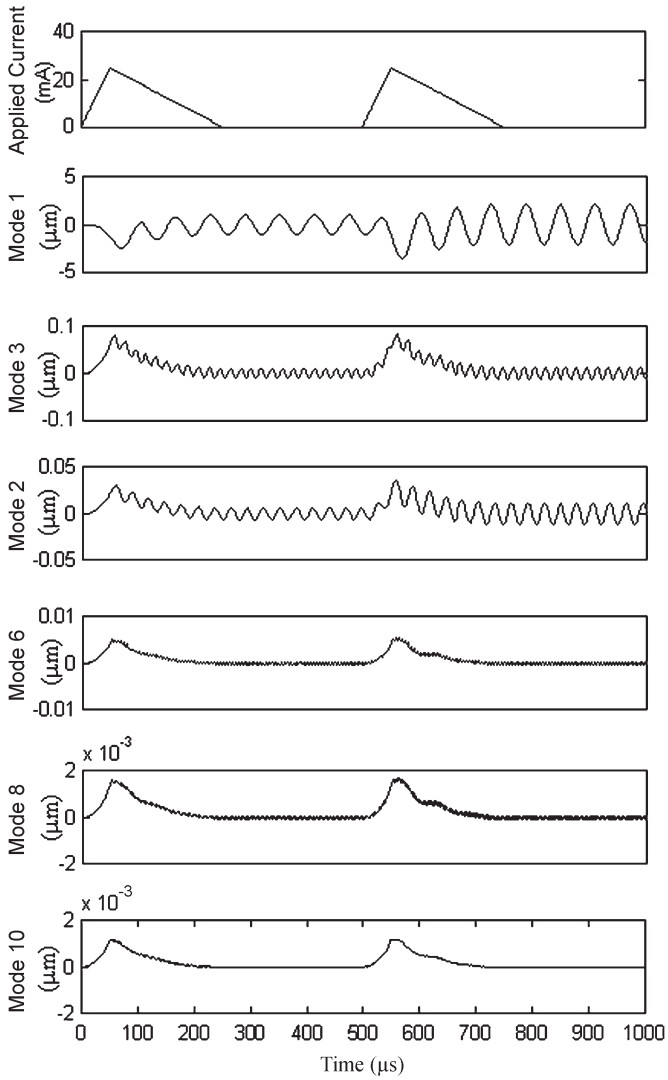

Fig. 6. Response to a 25-mA sawtooth wave with a 50-μs rise and a 500-μs period.

Figs. 5 and 6 show the dynamic responses of the force-macromodel coupled simulations. In Fig. 5, each mode response containing the ripple has the same timing as the applied square wave. In Fig. 6, mode 1 dominated the main response, while the rest reflected the general shape of the applied sawtooth wave. Each simulation took about 2 min. The results demonstrate that the generated macromodels achieved efficient modeling of the nonlinear coupling effects.

V. CONCLUSION

In this paper, we have proposed a macromodeling process for simulating a magnetic microactuator based on a FLM. Approaches, such as force and energy macromodels, have been utilized and discussed. Accordingly, macromodels have been efficiently established by using cluster estimation, gradient descent, and backpropagation. The required data for fitting the

macromodel have been also effectively reduced by using the proposed experimental design. Compared with quasi-static coupled simulations, the simulation of the force macromodel using the proposed FLM identification yields an error of less than 1.5% for a 5-μm displacement, demonstrating the effectiveness of the proposed scheme.

ACKNOWLEDGMENT

The authors would like to thank the anonymous reviewers for their valuable suggestions.

REFERENCES

[1] S. D. Senturia, "CAD challenges for microsensors, microactuators, and microsystems," *Proc. IEEE*, vol. 86, no. 8, pp. 1611–1626, Aug. 1998.
[2] N. R. Aluru and J. White, "A multilevel Newton method for mixed-energy domain simulation of MEMS," *J. Microelectromech. Syst.*, vol. 8, no. 3, pp. 299–308, Sep. 1999.
[3] L. D. Gabbay, J. E. Mehner, and S. D. Senturia, "Computer-aided generation of nonlinear reduced-order dynamic macromodels—I: Non-stress-stiffened case," *J. Microelectromech. Syst.*, vol. 9, no. 2, pp. 262–269, Jun. 2000.
[4] F. E. H. Tay, A. Ongkodjojo, and Y. C. Liang, "Backpropagation approximation approach based generation of macromodels for static and dynamic simulations," *Microsyst. Technol.*, vol. 7, no. 3, pp. 120–136, 2001.
[5] E. S. Hung and S. D. Senturia, "Generating efficient dynamical models for microelectromechanical systems from a few finite-element simulation runs," *J. Microelectromech. Syst.*, vol. 8, no. 3, pp. 280–289, Sep. 1999.
[6] S. Park and K. C. Lee, "A neural-network-based method of model reduction for the dynamic simulation of MEMS," *J. Micromech. Microeng.*, vol. 11, no. 3, pp. 226–233, 2001.
[7] T. Mukherjee, G. K. Fedder, D. Ramaswamy, and J. White, "Emerging simulation approached for micromachined devices," *IEEE Trans. Comput.-Aided Des. Integr. Circuits Syst.*, vol. 19, no. 12, pp. 1572–1588, Dec. 2000.
[8] C. T. Lin and C. S. George Lee, *Neural Fuzzy Systems/A Neuro-Fuzzy Synergism to Intelligent Systems*. Upper Saddle River, NJ: Prentice-Hall, 1996.
[9] S. L. Chiu, "A cluster estimation method with extension to fuzzy model with extension to fuzzy model identification," in *Proc. 3rd IEEE Conf. Fuzzy Systems*, Orlando, FL, 1994, vol. 2, pp. 1240–1245.
[10] J. C. Chiou and J. Y. Yang, "A CVD epitaxial deposition in a vertical barrel reactor: Process modeling using cluster-based fuzzy logic models," *IEEE Trans. Semicond. Manuf.*, vol. 11, no. 4, pp. 645–653, Nov. 1998.
[11] T. Takagi and M. Sugeno, "Fuzzy identification of systems and its application to modeling and control," *IEEE Trans. Syst., Man, Cybern.*, vol. SMC-15, no. 1, pp. 116–132, Feb. 1985.
[12] B. Schaible, H. Xie, and Y. C. Lee, "Fuzzy logic models for ranking process effects," *IEEE Trans. Fuzzy Syst.*, vol. 5, no. 4, pp. 545–556, Nov. 1997.
[13] H. Xie, R. L. Mahajan, and Y. C. Lee, "Fuzzy logic models for thermally based microelectronic manufacturing processes," *IEEE Trans. Semicond. Manuf.*, vol. 8, no. 3, pp. 219–227, Aug. 1995.
[14] L. Meirovitch, *Dynamics and Control of Structures*. New York: Wiley, 1992.
[15] J. Stoer and R. Bulirsch, *Introduction to Numerical Analysis*, 2nd ed. Berlin, Germany: Springer-Verlag, 1992.
[16] M. S. Phadke, *Quality Engineering Using Robust Design*. Englewood Cliffs, NJ: Prentice-Hall, 1989.
[17] R. R. Yager and D. P. Filev, "Unified structure and parameter identification of fuzzy models," *IEEE Trans. Syst., Man, Cybern.*, vol. 23, no. 4, pp. 1198–1205, Jul.–Aug. 1993.
[18] L. Wang and R. Langari, "Building Sugeno-type models using fuzzy discretization and orthogonal parameter estimations techniques," *IEEE Trans. Fuzzy Syst.*, vol. 3, no. 4, pp. 454–458, Nov. 1995.
[19] H. S. Hwang and K. B. Woo, "Linguistic fuzzy model identification," *Proc. IEE, Control Theory Appl.*, vol. 142, no. 6, pp. 537–544, 1995.
[20] C. H. Ko, J. J. Yang, and J. C. Chiou, "Efficient magnetic microactuator with an enclosed magnetic core," *J. Microlithogr. Microfabr. Microsyst.*, vol. 1, no. 2, pp. 144–149, 2002.
[21] D. J. Sadler, T. M. Liakopoulos, and C. H. Ahn, "A universal electromagnetic microactuator using magnetic interconnection concepts," *J. Microelectromech. Syst.*, vol. 9, no. 4, pp. 460–468, Dec. 2000.
[22] C. H. Ahn and M. G. Allen, "A fully integrated surface micromachined magnetic microactuator with a multilevel meander magnetic core," *J. Microelectromech. Syst.*, vol. 2, no. 1, pp. 15–22, Mar. 1993.

Chun-Hsu Ko was born in Tainan, Taiwan, R.O.C., in 1967. He received the M.S. degree in power mechanical engineering from National Tsing Hua University, Hsinchu, Taiwan, in 1991, and the Ph.D. degree in electrical and control engineering from National Chiao Tung University, Hsinchu, Taiwan, R.O.C., in 2003.

He worked at the Industrial Technology Research Institute, Taiwan, R.O.C., as an Assistant Researcher (1994–1998). He is presently an Assistant Professor in the Department of Computer Application Engineering, Far East College, Taiwan, R.O.C. His research interests include modeling and controlling of dynamic systems, fuzzy systems, and microelectromechanical systems.

Jin-Chern Chiou received the M.S. and Ph.D. degrees in aerospace engineering science from University of Colorado at Boulder, in 1986 and 1990, respectively.

He worked at the Center for Space Structure and Control, University of Colorado at Boulder, as a Research Associate (1991–1992), before joining the Department of Electrical and Control Engineering, National Chiao Tung University (NCTU), Taiwan, R.O.C., in 1992. His research interests include microelectromechanical systems (MEMS), fuzzy-logic modeling and control of chemical vapor deposition (CVD) process, servo control of compact disc-read only memory (CD-ROM) and DVD, and modeling and control of multibody dynamic systems (MBD). He is the coauthor of advanced reference books on CD-ROM system technology and mechanics and control of large flexible structures. Currently, Dr. Chiou possesses two U.S. and three R.O.C. patents.

Dr. Chiou has also obtained several awards from Acer Foundation, NCTU, and National Science Council, R.O.C., for his outstanding CD-ROM and MEMS research.